EDGE ARTICLE

Check for updates

All publication charges for this article have been paid for by the Royal Society of Chemistry

Site- and stereoselective silver-catalyzed intramolecular amination of electron-deficient heterobenzylic C–H bonds†

Tuan Anh Trinh, [ID] Stanislav Cherempei, Daniel S. Rampon and Jennifer M. Schomaker [ID] *

We report a method for the site- and stereoselective intramolecular amination of electron-deficient heterobenzylic C–H bonds *via* silver-catalyzed nitrene transfer (NT). A silver complex supported by a tripodal piperidine-based ligand afforded excellent reactivity under mild conditions (up to 96% yield), site-selectivity (up to >20 : 1), and diastereoselectivity (up to >20 : 1 dr) for the amination of heterobenzylic C–H bonds that reacted poorly with other metal-based catalysts for NT. Our catalyst proved highly amenable to substrates bearing diverse competing sites for functionalization, including complex molecules derived from pharmaceuticals and natural products. Ligand screening revealed the importance of scaffold rigidity, leading to the discovery of an analogous quinuclidine-based ligand that further improved the site-selectivity against tertiary C–H bonds in a handful of challenging substrates. The cyclic sulfamate products were readily converted into highly functionalized motifs containing nitrogen-based heterocycles and diverse functional groups. Mechanistic studies suggested a radical-based pathway displaying relatively low sensitivity towards the electronic profiles of the heterobenzylic C–H bond, which contributes to the excellent substrate tolerance of this method.
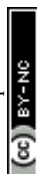
Introduction

Nitrogen heterocycles are a hallmark of active pharmaceutical ingredients (APIs), as nearly two-thirds of FDA-authorized small-molecule drugs contain at least one of these motifs.[1] Among the most prevalent aromatic heterocycles are electron-deficient *N*-heteroarenes, including pyridines, pyrimidines and quinolines. Reliable methods to functionalize molecules bearing these key heteroarenes are of significant interest to both synthetic and medicinal chemists. Their aliphatic amine counterparts also feature prominently in APIs, owing to the unique role of amines in modulating essential physiochemical and biological properties of pharmaceuticals, agrochemicals and other bioactive compounds.[2,3] As such, the enhanced therapeutic effects of existing drugs and the discovery of new drug candidates could benefit from incorporating amines into heteroaromatic compounds, particularly at heterobenzylic positions; indeed, these moieties are already found in several marketed pharmaceuticals (Scheme 1A).

Arguably, one of the most efficient routes to introduce an amine functionality at a heterobenzylic bond is to convert the targeted C–H bond directly to a new C–N bond.[4] While

Department of Chemistry, University of Wisconsin-Madison, Madison, Wisconsin 53706, USA. E-mail: schomakerj@chem.wisc.edu

† Electronic supplementary information (ESI) available. See DOI: https://doi.org/10.1039/d4sc08757g
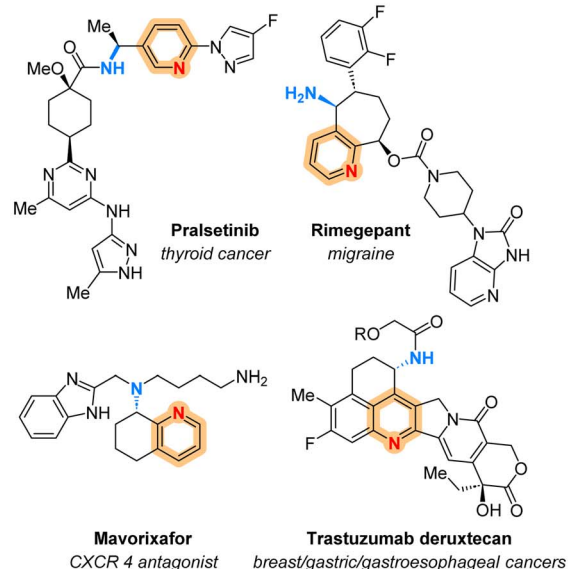
transition-metal catalyzed nitrene transfer (NT) is a powerful and well-established synthetic tool for aminating benzylic C–H bonds, an electron-poor *N*-heteroarene presents unique challenges. Firstly, the electrophilicity of a putative metal–nitrene species may render it polarity mismatched with an electron-deficient heterobenzylic C–H bond.[5] A second challenge is the propensity of a nucleophilic nitrogen atom(s) of the heteroarene to serve as a ligand for the metal, leading to deactivation of the catalyst if the binding is irreversible. The heteroaromatic nitrogen atom(s) may also react with the electrophilic nitrene precursors and hypervalent iodine reagents that are commonly employed in NT reactions[6,7] to generate undesirable *N*-imino heteroaromatic ylides[8–10] and other pyridinium adducts.[11] Unsurprisingly, precedents of NT into electron-deficient heterobenzylic C–H bonds are scarce (Scheme 1B). Che reported a single example of intramolecular amination into a benzylic C–H bond adjacent to a C3-substituted pyridine ring using an azide precursor and a catalytic iron-porphyrin/NHC complex; however, harsh conditions were required.[12] Meggers described NT of a *N*-benzyloxyurea-derived nitrene precursor into a (2-pyridyl)benzylic C–H bond using an iron–phenanthroline catalyst;[13] however, no examples bearing the alkyl chain on C3 or C4 of the pyridine ring or other electron-poor heterocycles were reported. Zhang aminated electron-deficient non-heterobenzylic C–H bonds, where the metalloradical reactivity of a cobalt-porphyrin complex alleviates the polarity mismatch.[14] Our group also disclosed one example of nitrene
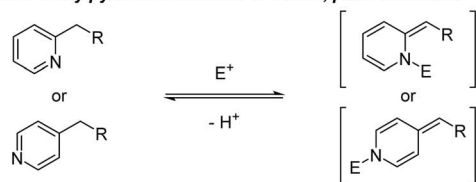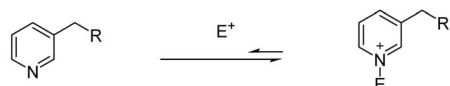
Scheme 1 Functionalization of electron-deficient C–H bonds.

insertion into a heterobenzylic C–H bond using a silver/bis(oxazoline) catalyst with a carbamate precursor in moderate yield.[15] Nonetheless, these examples do not reveal whether the highly site-selective amination of electron-poor heterobenzylic C–H bonds is achievable in the presence of inherently more reactive sites, including tertiary alkyl and other activated C–H bonds. On the other hand, oxygenations,[16–25] hydrazination,[26] halogenations,[27–30] thiolations,[27] and hetero-alkylations[31] at heterobenzylic C–H bonds have been reported, but rely on the polar activation of the resonance forms of 2- and 4-alkylpyridines. Meanwhile, strategies for reactions of 3-alkyl-pyridines are scarce, due to the lower acidity of their benzylic sites (Scheme 1C).[30,32] These limitations underscore the need for reliable, alternative methods to directly transform a broad range of heterobenzylic C–H bonds into valuable functional groups, particularly amines.

Herein, we report a silver-catalyzed protocol for site-selective intramolecular aminations of electron-deficient heterobenzylic C–H bonds *via* NT with sulfamates (Scheme 1D). We hypothesized that sulfamate-derived nitrene precursors would exhibit lower sensitivity to electronic effects and higher sensitivity towards the bond dissociation energies (BDE) of both activated

and unactivated C–H bonds, as compared to carbamates.[33] This difference in the behavior of the nitrene precursor could drive selective reaction at the electronically disfavored, yet weaker, heterobenzylic C–H bonds. Our method tolerates diverse heterocycles with different substitution patterns and displays exceptional chemo- and stereoselectivities, with moderate-to-excellent site-selectivities against an array of highly reactive competing C–H bonds, overriding the reactivity preferences seen with traditional catalysts for nitrene transfer.

Results and discussions

We commenced our studies by screening various combinations of silver salts and ligands against a handful of sulfamate-derived substrates (see Table S1 in the ESI† for further details). We found that the ligand denticity has a major impact on both conversion rates and mass balances of these reactions. Multidentate ligands provided moderate conversions and mass balances, as opposed to bidentate ligands, which had no reactivity.[34] Indeed, previous computations predicted a combination of a multidentate ligand-supported silver catalyst and a sulfamate precursor would be less sensitive to the C–H bond

electronics and favor reaction at weaker C–H bonds.[33] We also surmised that the multidenticity of the ligand would enforce stable coordination to the silver ion, thereby preventing competitive binding of the heteroarene substrate. To investigate selectivity parameters, we selected sulfamate **1a** bearing a competing tertiary C–H bond as a model substrate. Initial optimization studies explored the reaction of **1a** with AgOTf in CH_2Cl_2 using one of six multidentate *N*-ligands (**L1–L6**) (Table 1, entries 1–6). Mass balance and conversion were significantly higher with tetradentate ligands **L1–L5** (entries 1–5), as compared to the tridentate ligand **L6** (entry 6). The tertiary amine ligands **L1**, **L2** and *anti*-**L5** (entries 1–2 and 5) afforded higher selectivity for the heterobenzylic C–H amination product **2a** over the tertiary C–H amination product **3a**, as compared to the pentapyridyl ligands **L3** and **L4** (entries 3 and 4). These experimental results suggest that **L1**, **L2** and **L5** more effectively

enforce a transition-state geometry that strongly favors formation of a six-membered ring over a five-membered ring.[15] The higher yields and site-selectivity for **2a** when electron-donating groups (**L2**) or increased conformational rigidity (*anti*-**L5**) are introduced into the tris(2-pyridylmethyl)amine scaffold (**L1**) suggests enhancing the chelation ability of the ligand is beneficial.[35] As *anti*-**L5** provided the highest yield (86%), site- (>20 : 1 **2a** : **3a**), and stereoselectivity for **2a** (>20 : 1 *syn* : *anti*), this ligand was selected for solvent screening studies (entries 7–9). Gratifyingly, the use of anisole, a much less hazardous solvent than CH_2Cl_2,[36] afforded a 96% yield of **2a** with essentially no trace of **3a**, despite a slight decrease in diastereoselectivity (12.5 : 1 *syn* : *anti*) (entry 7). A stereoisomer of **L5**, where the two pyridine rings on the piperidine backbone are *cis* (*syn*-**L5**) instead of *trans* (*anti*-**L5**) to each other, furnished similar yield (95%) of **2a** with improved diastereoselectivity (18.5 : 1 *syn* : *anti*) (entry 10). Due to the greater ease of preparation and purification of *rac-syn*-**L5** over (*S,S,R*)-*anti*-**L5**, reaction of the former was carried out on a 2 mmol scale to deliver **2a** in 79% isolated yield (entry 11).

To validate the exceptional reactivity of our optimal reaction conditions, results were benchmarked against selected catalysts commonly employed in NT reactions, particularly those utilizing sulfamate precursors. Treatment of **1a** with previously reported rhodium-,[37] copper-,[38] iron-[39] and manganese-catalyzed[40] protocols resulted in poor yields of **2a**/**3a** and significant amounts of recovered **1a** (Table 2, (A)), suggesting that the corresponding catalysts were deactivated by substrate inhibition. The desired product **2a** was obtained in either low site-selectivity (under Rh- and Cu-catalyzed conditions) or as a minor regioisomer (under Fe- and Mn-catalyzed conditions). Other reported NT protocols that employ sulfamoyl azides (with Zhang's cobalt-porphyrin catalyst)[14] and ureas (with Meggers' iron–phenanthroline catalyst)[13] also failed to provide the respective pyridine-containing products (Table 2, (B)), despite their excellent performances with related substrates as shown in Scheme 1B. Specifically, the former reaction presumably suffered catalyst deactivation, and the latter only resulted in decomposition of starting material.

With the optimized conditions in hand, we investigated the substrate scope of the reaction, starting with the heteroaromatic moiety (Table 3). Excellent yields and selectivities (>20 : 1 rr, dr) were observed with a range of *para*-C6-electron-donating and withdrawing groups (**2b–2f**). Interestingly, benchmarking studies carried out with **2d** and **2f** using Rh, Cu, and Mn catalysts revealed that their reactivity was heavily dependent on the electronics of the heteroaromatic ring. The presence of a more electron-rich pyridine ring in **2d** improves reactivity at the expense of mass balance, while the electron-poor pyridine ring of **2f** erodes the desired site-selectivity in favor of the formation of **3f**. These results highlight another advantage of our Ag-catalyzed protocol over other metals, as it is capable of achieving the efficient functionalizations of heterobenzylic C–H bonds with diverse electronic profiles.

A lack of steric shielding of the N-atom in substrates lacking C6 substitution on the pyridine ring, which is particularly problematic for the benchmarking catalysts, did not cause substrate inhibition of the Ag catalyst. The presence of a substituent at the

Table 1 Optimization studies[a]

Entry	Ligand	Solvent	2a yield	3a yield	RSM
1	**L1**	CH_2Cl_2	66% (*syn* : *anti* = 19.2 : 1)	3%	7%
2	**L2**	CH_2Cl_2	82% (*syn* : *anti* = 9.3 : 1)	4%	<1%
3	**L3**	CH_2Cl_2	71% (*syn* : *anti* = 4.1 : 1)	12%	<1%
4	**L4**	CH_2Cl_2	54% (*syn* : *anti* = 3.4 : 1)	30%	<1%
5	*anti*-**L5**	CH_2Cl_2	86% (*syn* : *anti* = 21.3 : 1)	3%	<1%
6	**L6**	CH_2Cl_2	41% (*syn* : *anti* = 8.9 : 1)	5%	12%
7	*anti*-**L5**	PhOMe	**96% (*syn* : *anti* = 12.5 : 1)**	**<1%**	**4%**
8	*anti*-**L5**	^iPrOAc	32% (*syn* : *anti* = 13.3 : 1)	<1%	60%
9	*anti*-**L5**	PivCN	61% (*syn* : *anti* = 15.4 : 1)	<1%	32%
10	*syn*-**L5**	PhOMe	**95% (*syn* : *anti*= 18.5 : 1)**	**<1%**	**<1%**
11[b]	*syn*-**L5**	PhOMe	79% (*syn* : *anti*> 20 : 1)[c]	<1%	<1%
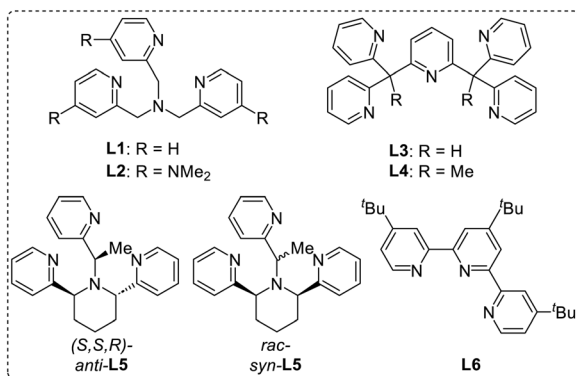
[a] Reactions were carried out on a 0.1 mmol scale unless otherwise noted. Yields and diastereomeric ratios were determined by ^1H NMR analysis of crude product mixtures using 1,3,5-trimethoxybenzene as an internal standard. [b] 2 mmol scale, 0.2 M PhOMe. [c] Isolated yield.

Table 2 Benchmarking studies using previously reported nitrene transfer conditions with sulfamate substrates

A. Benchmarking studies with sulfamate-derived nitrene precursors

54% RSM	Condition A	18% (5.6:1 dr)	5%
57% RSM	Condition B	4%	<1%
51% RSM	Condition C	<1%	33%
<44% RSM	Condition D	<20%	<36%

Condition A:
Rh$_2$esp$_2$ (5 mol%), PhI(OAc)$_2$ (1.1 eq.), MgO (2.3 eq.), CH$_2$Cl$_2$ (0.16 M), 40 °C, 4 h
Du Bois, 2001

Condition B:
[Cu(MeCN)$_4$]PF$_6$ /phen (10 mol%) PhIO (1.3 eq.), 4 Å MS (25 mg), MeCN (0.1 M), 45 °C, 18 h
Nicholas, 2011

Condition C:
[Fe(Pc)]Cl (10 mol%) AgSbF$_6$ (10 mol%) PhI(OPiv)$_2$ (1.2 eq.) PhMe/MeCN (4:1 v/v, 0.5 M), rt, 16 h
White, 2012

Condition D:
[Mn(^{t}BuPc)]Cl (10 mol%) AgSbF$_6$ (10 mol%) PhI(OPiv)$_2$ (1.2 eq.), 4 Å MS (25 mg), PhH/MeCN (9:1 v/v, 0.5 M), rt, 16 h
White, 2015

B. Benchmarking studies with other nitrene precursors

Condition E:
Co(3,5-Di^{t}Bu-IbuPhyrin (2 mol%), C$_6$H$_6$ (0.1 M), N$_2$, 40 °C, 24 h
Zhang, 2012

53% RSM → <1%

Condition F:
FeCl$_2$·4H$_2$O (10 mol%) phen (20 mol%), Na$_2$CO$_3$ (3 eq.), MeCN (0.1 M), 50 °C, 20 h
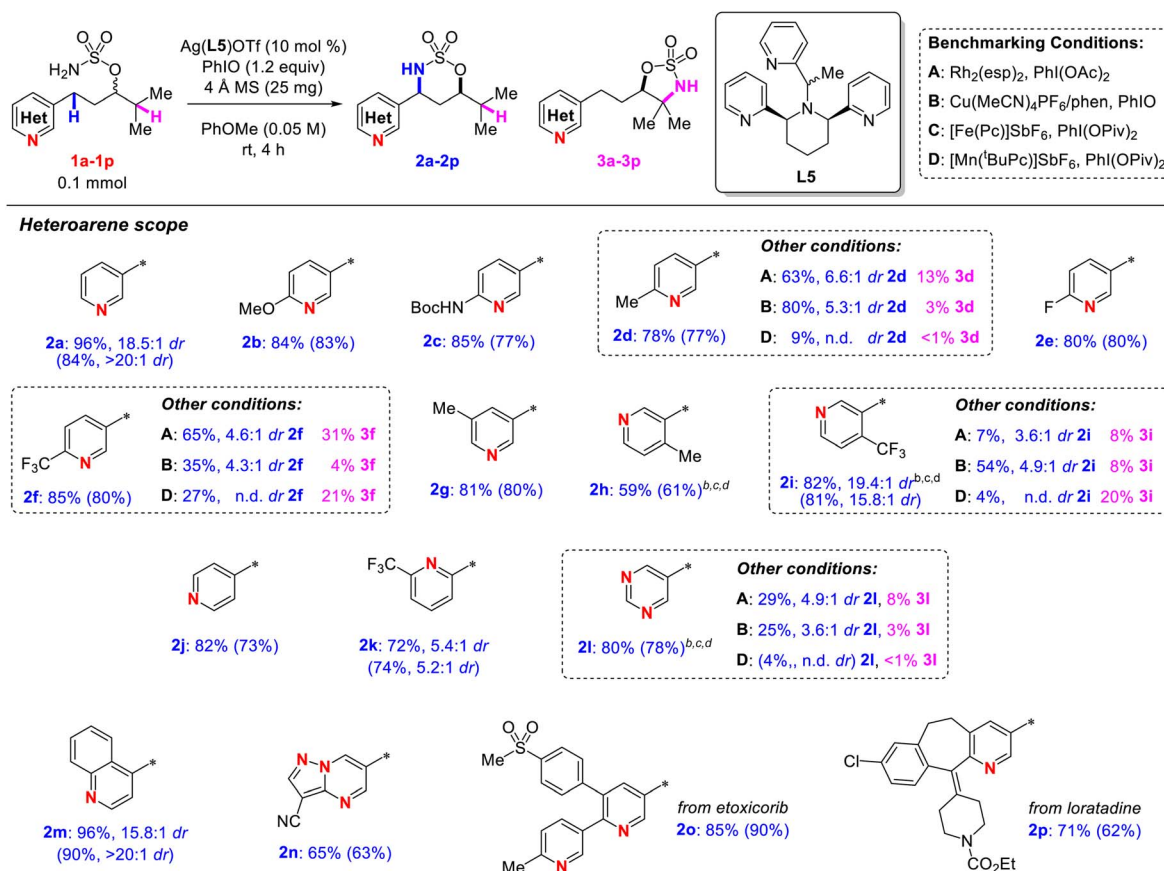*Meggers, 2021*

<1% RSM → <1%
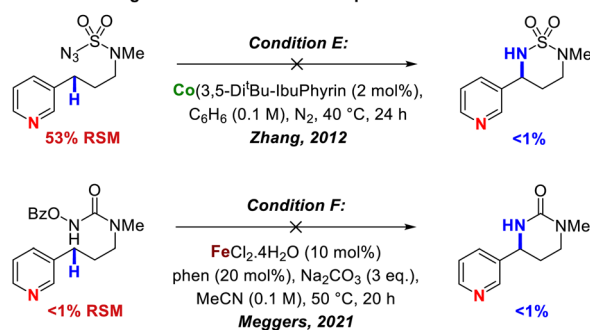
meta-C5-position did not affect the reactivity (**2g**). Reactions also proceeded smoothly with *ortho*-C4-substitutions (**2h–2i**), despite the requirement for increased loadings of catalyst and oxidant to ensure complete conversion within a reasonable period of time. It is worth noting that for **2i**, the reaction outcomes were still excellent in the presence of an electronically deactivating and sterically encumbered *ortho*-CF$_3$ group. Conversely, the Rh and Mn catalysts favored the other regioisomer **3i**, along with <10% yield of **2i**, while the Cu catalyst gave lower yield and selectivities. The 4- and 2-alkylpyridines (**2j–2k**) were also aminated in excellent yields using the Ag catalyst; however, the 2-alkylpyridine **2k** gave lower dr and required C6 substitution to improve the mass balance. The reaction also tolerated diverse electron-deficient heteroarenes of medicinal interest (pyrimidine, quinoline, pyrazolo[1,5-*a*]pyrimidine) (**2l–2n**) and pharmaceutical-derived substrates (**2o–2p**) to afford the corresponding products in good-to-excellent yields and selectivities.

The aliphatic side chain was varied to examine the site-selectivity in the presence of other types of competing C–H

bonds (Table 4, top). The preference for heterobenzylic C–H amination was good-to-excellent against unactivated secondary C–H bonds of the same tether length, regardless of side-chain structures or statistical control (**2q–2s**). In some cases, decreased conversions and site-selectivities under standard conditions were overcome by lowering the reaction temperature (**2q**) or changing the solvent (**2r**). In the presence of competing tertiary C–H bonds of the same tether length, the desired site-selectivity decreased, but still favored the electron-poor C–H in most cases to give the corresponding products in moderate-to-excellent yields (**2t–2aa**). This contrasts to benchmarking studies employing other metal catalysts (**1t–1v** and **1x–1y**). For instance, the use of Rh catalysis overwhelmingly favored amination at the tertiary sites with low yields (<10%) of the desired heterobenzylic amination. Under our Ag-catalyzed conditions, site-selectivity against non-cyclic tertiary C–H bonds was not affected by the position of branching in the alkyl chain and showed an increase from 1.9 : 1 (**2t** and **2v**) to 5.9 : 1 when a bulky, inductively withdrawing group is proximal to the tertiary C–H bond (**2u**). Notably, the formation of **2v** was exclusively *anti*-stereoselective, as opposed to the *syn*-stereoselectivity in C3-branched products. Against tertiary C–H bonds in simple cyclic systems, the product distribution displayed a close correlation with the predicted BDEs.[41] In these cases, the desired regioisomers were obtained in ratios of 2.1 : 1, 1 : 1.1, and 2.8 : 1 against cyclobutyl (**2w**), cyclopentyl (**2x**), and cyclohexyl (**2y**) tertiary C–H bonds, respectively. To our delight, the product ratios improved remarkably in more complex substrates. In the presence of a competing cyclohexyl tertiary C–H bond, **2z** was almost exclusively obtained in 96% yield and excellent dr. Product **2aa** was also obtained in good yield and site-selectivity (3.0 : 1) against a competing cyclopentyl tertiary C–H bond. On the other hand, the heterobenzylic amination was considerably less site-selective against simple allylic (**2ab**, 1 : 1.6 rr), propargylic (**2ac**, 1 : 1.6 rr), and benzylic (**2ad**, 1 : 3.3 rr) C–H bonds, which have similar bond strengths and are more electronically favored. Despite this persistent challenge, the desired products were still obtained in moderate yields that were significantly higher than those obtained with Rh$_2$(esp)$_2$. The reaction again proved to perform better with a complex substrate, as **2ae** was obtained in good yield and site-selectivity (4.0 : 1) in the presence of a competing tertiary, allylic C–H bond. These results indicate that the Ag catalyst not only selects for weak C–H bonds, but also provides excellent steric discrimination when multiple sites of similar BDEs are present in the same molecule. Finally, products derived from a primary sulfamate (**2af**, 3 mmol scale) and a tertiary heterobenzylic C–H bond-containing precursor (**2ag**) were obtained in good yields.

To further improve the site-selectivity for amination of heterobenzylic against tertiary C–H bonds *via* catalyst control, another round of catalyst screening was conducted on substrate **1t** under the standard reaction conditions (see Table S2 in the ESI† for further details). In terms of the silver salt, AgBF$_4$ improved the yield of **2t** from 56% to 64% and thus was used for subsequent ligand screening. We attributed this improvement to the further attenuation of electrophilicity of the silver–nitrene complex that results from a stronger electrostatic
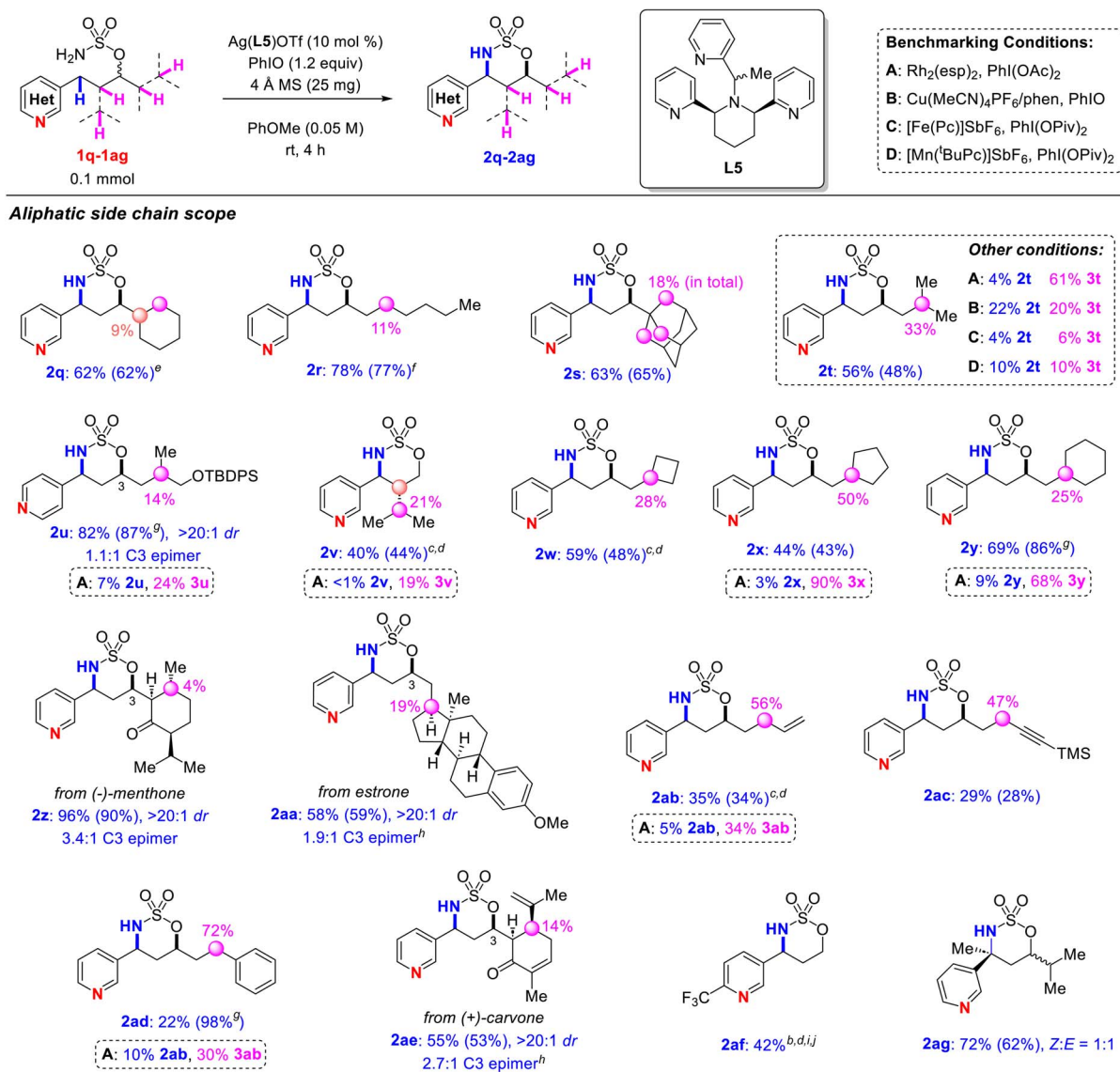
Table 3 Substrate scope for the amination of heterobenzylic C–H bonds in diverse heteroarenes[a]

Heteroarene scope

2a: 96%, 18.5:1 dr
(84%, >20:1 dr)

2b: 84% (83%)

2c: 85% (77%)

2d: 78% (77%)
Other conditions:
A: 63%, 6.6:1 dr **2d** 13% **3d**
B: 80%, 5.3:1 dr **2d** 3% **3d**
D: 9%, n.d. dr **2d** <1% **3d**

2e: 80% (80%)

2f: 85% (80%)
Other conditions:
A: 65%, 4.6:1 dr **2f** 31% **3f**
B: 35%, 4.3:1 dr **2f** 4% **3f**
D: 27%, n.d. dr **2f** 21% **3f**

2g: 81% (80%)

2h: 59% (61%)[b,c,d]

2i: 82%, 19.4:1 dr[b,c,d]
(81%, 15.8:1 dr)
Other conditions:
A: 7%, 3.6:1 dr **2i** 8% **3i**
B: 54%, 4.9:1 dr **2i** 8% **3i**
D: 4%, n.d. dr **2i** 20% **3i**

2j: 82% (73%)

2k: 72%, 5.4:1 dr
(74%, 5.2:1 dr)

2l: 80% (78%)[b,c,d]
Other conditions:
A: 29%, 4.9:1 dr **2l**, 8% **3l**
B: 25%, 3.6:1 dr **2l**, 3% **3l**
D: (4%,, n.d. dr) **2l**, <1% **3l**

2m: 96%, 15.8:1 dr
(90%, >20:1 dr)

2n: 65% (63%)

2o: 85% (90%) *from etoxicorib*

2p: 71% (62%) *from loratadine*

Benchmarking Conditions:
A: Rh$_2$(esp)$_2$, PhI(OAc)$_2$
B: Cu(MeCN)$_4$PF$_6$/phen, PhIO
C: [Fe(Pc)]SbF$_6$, PhI(OPiv)$_2$
D: [Mn(^{t}BuPc)]SbF$_6$, PhI(OPiv)$_2$

[a] Isolated yields in parentheses. rr, dr > 20 : 1 unless otherwise noted. [b] 15 mol% Ag(L5)OTf. [c] 1.5 equiv. PhIO. [d] 16 h.
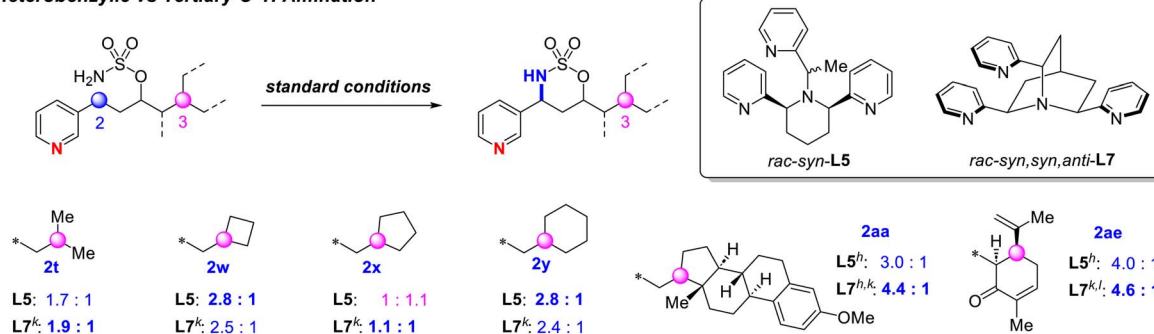
interaction between the cationic silver–ligand complex and the smaller BF$_4$ anion, which in turn favors NT at the less electron-rich C–H bond. After screening a variety of tris(pyridyl)amine-type ligands, we found conformational rigidity had a critical impact on both the overall yield and product ratio. Interestingly, while the ligands with a non-cyclic scaffold (**L1** and **L2**) resulted in a decreased **2t**/**3t** ratio of 1.3 : 1, simply removing the pendant methyl group from *syn*-**L5** led to an even more significant loss of site-selectivity (Table S2†). Attempts to replace the methyl group with larger groups were unsuccessful; thus, we envisaged replacing the piperidine backbone with a quinuclidine scaffold (**L7**) to enhance the conformational rigidity of the ligand. **L7** contains a (*syn*,*syn*,*anti*) relative stereochemistry of the pyridine arms, rendering its coordination geometry comparable to that of *syn*-**L5** (Table 3, bottom). Despite slightly lower conversions as compared to those observed with AgOTf/*syn*-**L5** at the same reaction times, AgBF$_4$/**L7** delivered comparable product ratios among the simple substrates, with a noticeable improvement in the reaction of **1x** to give **2x** as the major regioisomer. We were pleased to observe other striking improvements in site-selectivity when AgBF$_4$/**L7** was employed with more complex substrates; for example, the selectivity for **2aa** and **2ae** increased to 4.4 : 1 and 4.6 : 1, respectively (Table 3, bottom). We surmised

that the decreased flexibility of the coordination sphere associated with **L7** raises the energy barrier for nitrene insertion into the more sterically congested tertiary site to a larger extent as compared to reaction at the heterobenzylic site. However, attempts to facilitate steric discrimination *via* the installation of bulky substituents, such as mesityl, on the pyridine rings of *syn*-**L5**, reversed the site-selectivity for **2t** to favor tertiary insertion in **3t** (Table S2†). This reversal was attributed to intramolecular repulsion and displacement of at least one of the ligand arms of the Ag complex from the substrate, deactivating the hetero-benzylic C–H bond towards NT. This result further underscores the importance of scaffold rigidity to balance steric discrimination and stabilization of metal–ligand interactions. To probe the effects of substrate–ligand non-covalent interactions on inducing the site-selectivity,[42] screening of aromatic solvents across a wide range of dielectric constants was performed using AgBF$_4$/*syn*-**L5** as the catalyst (see Table S2 in the ESI† for further details). An inverse correlation between the dielectric constants and the observed site-selectivity ratios was observed. We speculate that the excellent reactivity and selectivity resulting from the use of anisole as a solvent are due to both its superior solubilizing effects and relative non-polarity compared to dichloromethane and other aromatic solvents. The latter factor

Table 4 Substrate scope for amination with different aliphatic side chains[a]

Aliphatic side chain scope

2q: 62% (62%)[e]

2r: 78% (77%)[f]

2s: 63% (65%)

2t: 56% (48%)

Other conditions:
A: 4% **2t**, 61% **3t**
B: 22% **2t**, 20% **3t**
C: 4% **2t**, 6% **3t**
D: 10% **2t**, 10% **3t**

2u: 82% (87%[g]), >20:1 *dr*
1.1:1 C3 epimer
A: 7% **2u**, 24% **3u**

2v: 40% (44%)[c,d]
A: <1% **2v**, 19% **3v**

2w: 59% (48%)[c,d]
A: 3% **2x**, 90% **3x**

2x: 44% (43%)
A: 3% **2x**, 90% **3x**

2y: 69% (86%[g])
A: 9% **2y**, 68% **3y**

from (-)-menthone
2z: 96% (90%), >20:1 *dr*
3.4:1 C3 epimer

from estrone
2aa: 58% (59%), >20:1 *dr*
1.9:1 C3 epimer[h]

2ab: 35% (34%)[c,d]
A: 5% **2ab**, 34% **3ab**

2ac: 29% (28%)

2ad: 22% (98%[g])
A: 10% **2ab**, 30% **3ab**

from (+)-carvone
2ae: 55% (53%), >20:1 *dr*
2.7:1 C3 epimer[h]

2af: 42%[b,d,i,j]

2ag: 72% (62%), *Z:E* = 1:1

Heterobenzylic vs Tertiary C–H Amination

*rac-syn-**L5***

*rac-syn,syn,anti-**L7***

2t	**2w**	**2x**	**2y**	**2aa**	**2ae**
L5: 1.7 : 1	L5: 2.8 : 1	L5: 1 : 1.1	L5: 2.8 : 1	L5[h]: 3.0 : 1	L5[h]: 4.0 : 1
L7[k]: 1.9 : 1	L7[k]: 2.5 : 1	L7[k]: 1.1 : 1	L7[k]: 2.4 : 1	L7[h,k]: 4.4 : 1	L7[k,l]: 4.6 : 1

[a] Isolated yields in parentheses. rr, dr > 20 : 1 unless otherwise noted. [b] 15 mol% Ag(**L5**)OTf. [c] 1.5 equiv. PhIO. [d] 16 h. [e] 75% yield at 0 °C after 40 h. [f] CH₂Cl₂ as solvent. [g] Total yield, inseparable regioisomeric mixture. [h] 0.025 mmol scale. [i] 2.0 equiv. PhIO. [j] 3.0 mmol scale, 0.2 M PhOMe. [k] AgBF₄ was used instead of AgOTf. [l] 0.0125 mmol scale.
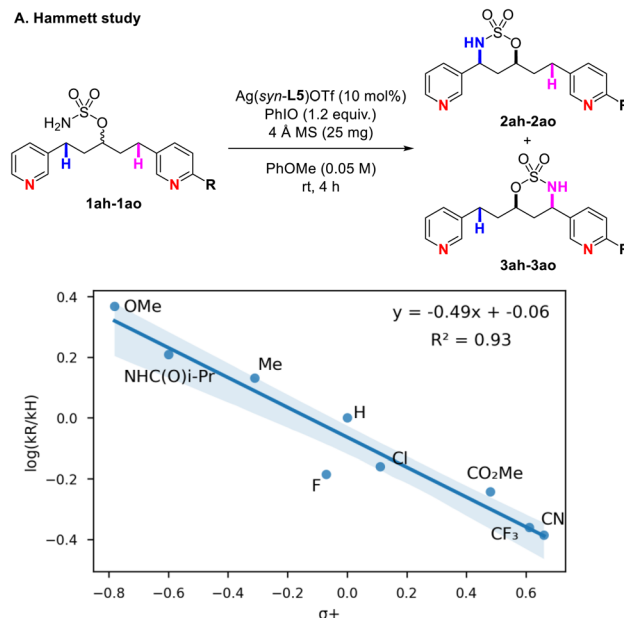
presumably enhances the attractive π–π and dispersion interactions between the heterocyclic substrate and ligand that are essential to inducing the site-selectivity for amination at the heterobenzylic C–H bond.[42]
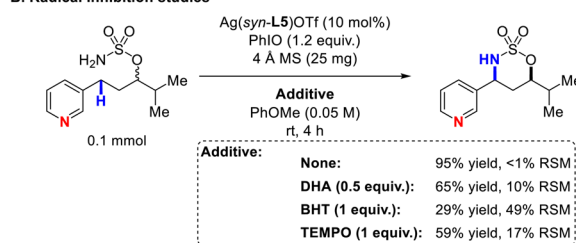
The heteroarene-containing sulfamates are convenient building blocks; examples of post-functionalizations are shown in Scheme 2. The nitrogen of **2af** was protected with a Cbz group to afford **4** in 61% yield. This intermediate can readily be ring-opened with various nucleophiles, including water, azide, morpholine and fluoride, to obtain the corresponding 1,3-functionalized products (**5–8**) in moderate-to-excellent yields (Scheme 2A). Reactions of disubstituted cyclic sulfamate **2t** required more forcing conditions; Cbz-protection followed by treatment with AcOK in DMSO at 80 °C furnished *N*-Cbz-1,3-aminoketone (**9**) in 27% yield over 2 steps (Scheme 2B). This sequence can potentially provide efficient access to all four diastereomers of the corresponding 1,3-aminoalcohol, depending on the absolute stereochemistry of the C–O bond before the aminative cyclization step and after reduction of the ketone resulting from the deprotonative ring-opening step.

To gain insight into the potential mechanistic differences of this chemistry compared to previous NT systems, a Hammett study was conducted with substrates containing competing heterobenzylic C–H bonds (**1ah–1ao**, Scheme 3A). A reasonably linear correlation ($R^2 = 0.93$) between $\log(k_R/k_H)$ and the σ^+ Hammett constants was noted, with a ρ-value of −0.49. This ρ_σ^+-value is less negative than those of the benchmarked sulfamate-based NT reactions (Ag(**L1**)OTf:[42] −0.69; Rh catalyst:[43] −0.55; Fe catalyst:[40] −1.12; Mn catalyst:[40] −0.88) and several other systems employing diverse catalysts and nitrene precursors (between −1.49 and −0.66).[44–51] This result suggests that the Ag-catalyzed reaction has a relatively low sensitivity to the electronic effects
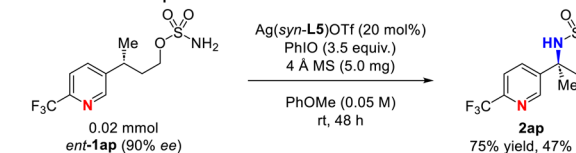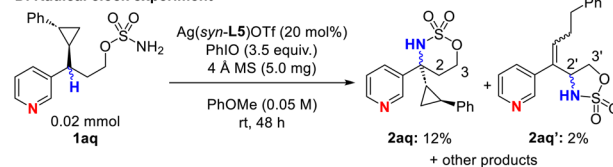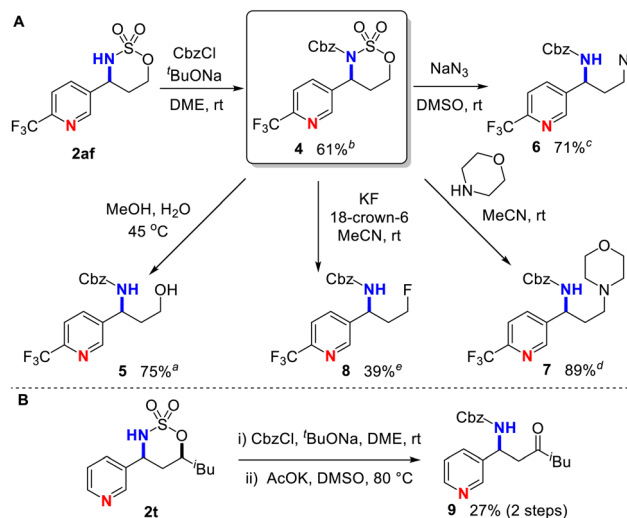

Scheme 3 Mechanistic studies. Yields were determined by ^{1}H NMR analysis of crude mixtures.

on the heterobenzylic C–H bond. To determine whether the reaction undergoes a concerted or stepwise mechanism, radical trapping experiments were conducted. After subjecting **1a** to the standard reaction conditions in the presence of 1 equivalent of TEMPO, 1 equivalent of butylated hydroxytoluene (BHT) or 0.5 equivalent of 9,10-dihydroanthracene (DHA), respectively (Scheme 3B), substantial losses of yield and mass balances were noted, although detection and isolation of any trapped products proved challenging under the reaction conditions. Notably, these results contrast with our previous observations that addition of DHA does not affect the amination of non-heteroaromatic benzylic C–H bonds using Ag(**L5**)OTf.[35] While

Scheme 2 Synthetic applications of pyridine-containing cyclic sulfamates. Nucleophilic ring-opening reactions were carried out on a 0.1 mmol scale unless otherwise indicated. [a]0.313 mmol scale. Conditions: [b]CbzCl (2.5 equiv.), [t]BuONa (1.5 equiv.), DME (0.1 M), rt, overnight; [c]NaN₃ (2 equiv.), DMSO (0.2 M), rt, overnight; [d]Morpholine (1.1 equiv.), MeCN (0.2 M), rt, overnight; [e]KF (2 equiv.), 18-crown-6 (1 equiv.), MeCN (0.2 M), rt, 48 h.

these results imply a heterobenzylic radical intermediate results from hydrogen atom transfer (HAT) to the Ag-nitrene species, we did not rule out a possibility that the radical scavengers impact the outcome by reacting with the oxidant. To further probe the intermediacy and relative lifetime of a heterobenzylic radical, a stereoretention experiment was performed with **1ap**, which contains an enantioenriched tertiary heterobenzylic C–H bond (90% ee) (Scheme 3C). After complete conversion, the corresponding product **2ap** was obtained with a significant loss of ee (47% ee). The partial racemization indicates the reaction indeed proceeds *via* a stabilized heterobenzylic radical intermediate following the initial HAT step, which then racemizes at a non-negligible rate relative to that of a product-forming radical rebound (RR) step. This result differs from our mechanistic findings in previous Ag-catalyzed NT systems, where the reactions are proposed to undergo a stepwise radical pathway involving barrierless RR,[42] evidenced by the observation of complete stereoretention.[35] In a radical clock experiment (Scheme 3D), small amount(s) of cyclopropane-ring opening product(s) were detected when a cyclopropane moiety is adjacent to the heterobenzylic site, further corroborating the intermediacy of a heterobenzylic radical.

In conclusion, we have developed a highly chemo-, site-, and stereoselective method to aminate electron-deficient heterobenzylic C–H bonds *via* silver-catalyzed intramolecular nitrene transfer. Key to enabling this challenging transformation is the catalyst-controlled alleviation of polarity mismatch and circumvention of substrate inhibition. Optimization of ligand design revealed the importance of conformational rigidity to improving the site-selectivity against other reactive C–H bonds. This protocol demonstrates exceptional tolerance of several heteroaromatic compounds, including those derived from drugs and natural products that represent a coveted yet elusive chemical space for traditional metal catalysts.

Data availability

The data supporting this article have been included as part of the ESI.†

Author contributions

The manuscript was written through contributions of all authors. All authors have given approval to the final version of the manuscript.

Conflicts of interest

There are no conflicts to declare.

Acknowledgements

References

1 E. Vitaku, D. T. Smith and J. T. Njardarson, Analysis of the Structural Diversity, Substitution Patterns, and Frequency of Nitrogen Heterocycles among U.S. FDA Approved Pharmaceuticals, *J. Med. Chem.*, 2014, **57**, 10257–10274.

2 S. A. Lawrence, *Amines: Synthesis, Properties, and Applications*, Cambridge University Press, Cambridge, 2004.

3 T. Henkel, R. M. Brunne, H. Müller and F. Reichel, Statistical Investigation into the Structural Complementarity of Natural Products and Synthetic Compounds, *Angew. Chem., Int. Ed.*, 1999, **38**(5), 643–647.

4 F. Collet, R. H. Dodd and P. Dauban, Catalytic C–H Amination: Recent Progress and Future Directions, *Chem. Commun.*, 2009, **34**, 5061–5074.

5 D. Hazelard, P.-A. Nocquet and P. Compain, Catalytic C–H Amination at Its Limits: Challenges and Solutions, *Org. Chem. Front.*, 2017, **4**, 2500–2521.

6 A. Yoshimura and V. V. Zhdankin, Advances in Synthetic Applications of Hypervalent Iodine Compounds, *Chem. Rev.*, 2016, **116**, 3328–3435.

7 K. Kiyokawa, S. Nakamura, K. Jou, K. Iwaida and S. Minakata, Transition-Metal-Free Intramolecular C−H Amination of Sulfamate Esters and N-Alkylsulfamides, *Chem. Commun.*, 2019, **55**, 11782–11785.

8 R. A. Abramovitch and T. Takaya, Reaction of Sulfonyl Azides with Pyridines and Fused Pyridine Derivatives, *J. Org. Chem.*, 1972, **37**, 2022–2029.

9 S. L. Jain, V. B. Sharma and B. Sain, Copper-Catalyzed Imination of Pyridines Using PhI=NTs as Nitrene Precursor, *Tetrahedron Lett.*, 2003, **44**, 4385–4387.

10 Y. Jiang, G.-C. Zhou, G.-L. He, L. He, J.-L. Li and S.-L. Zheng, Ruthenium(II)-Porphyrin Catalyzed Selective *N*-Imidation of Aromatic Nitrogen Heterocycles, *Synthesis*, 2007, **10**, 1459–1464.

11 R. Weiss, Electrostatic Activation of Hypervalent Organo-Iodine Compounds: Bis(onio)-Substituted Aryliodine(III) Salts, *Angew. Chem., Int. Ed.*, 1994, **33**, 891–893.

12 K.-P. Shing, Y. Liu, B. Cao, X.-Y. Chang, T. You and C.-M. Che, *N*-Heterocyclic Carbene Iron(III) Porphyrin-Catalyzed Intramolecular C(sp^3)-H Amination of Alkyl Azides, *Angew. Chem., Int. Ed.*, 2018, **57**, 11947–11951.

13 L. Jarrige, Z. Zhou, M. Hemming and E. Meggers, Efficient Amination of Activated and Non-Activated C(sp^3)−H Bonds with a Simple Iron–Phenanthroline Catalyst, *Angew. Chem., Int. Ed.*, 2021, **60**, 6314–6319.

14 H. Lu, Y. Hu, H. Jiang, L. Wojtas and X. P. Zhang, Stereoselective Radical Amination of Electron-Deficient C(sp^3)–H Bonds by Co(II)-Based Metalloradical Catalysis:

Direct Synthesis of α-Amino Acid Derivatives *via* α-C–H Amination, *Org. Lett.*, 2012, **14**, 5158–5161.

15 M. Ju, M. Huang, L. E. Vine, M. Dehghany, J. M. Roberts and J. M. Schomaker, Tunable Catalyst-Controlled Syntheses of β- and γ-Amino Alcohols Enabled by Silver-Catalysed Nitrene Transfer, *Nat. Catal.*, 2019, **2**, 899–908.

16 J. Liu, X. Zhang, H. Yi, C. Liu, R. Liu, H. Zhang, K. Zhuo and A. Lei, Chloroacetate-Promoted Selective Oxidation of Heterobenzylic Methylenes under Copper Catalysis, *Angew. Chem., Int. Ed.*, 2015, **54**, 1261–1265.

17 L. Ren, L. Wang, Y. Lv, G. Li and S. Gao, Synergistic H_4NI–AcOH Catalyzed Oxidation of the $C(sp^3)$–H Bonds of Benzylpyridines with Molecular Oxygen, *Org. Lett.*, 2015, **17**, 2078–2081.

18 D. P. Hruszkewycz, K. C. Miles, O. R. Thiel and S. S. Stahl, Co/NHPI-Mediated Aerobic Oxygenation of Benzylic C–H Bonds in Pharmaceutically Relevant Molecules, *Chem. Sci.*, 2017, **8**, 1282–1287.

19 W. Jin, P. Zheng, W. Wong and G. Law, Efficient Selenium-Catalyzed Selective $C(sp^3)$–H Oxidation of Benzylpyridines with Molecular Oxygen, *Adv. Synth. Catal.*, 2017, **359**, 1588–1593.

20 H. Sterckx, C. Sambiagio, V. Médran-Navarrete and B. U. W. Maes, Copper-Catalyzed Aerobic Oxygenation of Benzylpyridine *N*-Oxides and Subsequent Post-Functionalization, *Adv. Synth. Catal.*, 2017, **359**, 3226–3236.

21 T. Abe, S. Tanaka, A. Ogawa, M. Tamura, K. Sato and S. Itoh, Copper-Catalyzed Selective Oxygenation of Methyl and Benzyl Substituents in Pyridine with O_2, *Chem. Lett.*, 2017, **46**, 348–350.

22 C. Zhu, H. Li and C. Chu, Direct $C(sp^3)$-H Functionalization of 2-Methylazaarenes Using 4-Substituted-TEMPO, *Tetrahedron Lett.*, 2018, **59**, 4454–4457.

23 H. Wang, J. Liu, J.-P. Qu and Y.-B. Kang, Overcoming Electron-Withdrawing and Product-Inhibition Effects by Organocatalytic Aerobic Oxidation of Alkylpyridines and Related Alkylheteroarenes to Ketones, *J. Org. Chem.*, 2020, **85**, 3942–3948.

24 J. C. Cooper, C. Luo, R. Kameyama and J. F. Van Humbeck, Combined Iron/Hydroxytriazole Dual Catalytic System for Site Selective Oxidation Adjacent to Azaheterocycles, *J. Am. Chem. Soc.*, 2018, **140**, 1243–1246.

25 M. Kaur, J. C. Cooper and J. F. Van Humbeck, Site-Selective Benzylic C–H Hydroxylation in Electron-Deficient Azaheterocycles, *Org. Biomol. Chem.*, 2024, **22**, 4888–4894.

26 K. W. Bentley, K. A. Dummit and J. F. Van Humbeck, A Highly Site-Selective Radical sp^3 C–H Amination of Azaheterocycles, *Chem. Sci.*, 2018, **9**, 6440–6445.

27 M. Meanwell, B. S. Adluri, Z. Yuan, J. Newton, P. Prevost, M. B. Nodwell, C. M. Friesen, P. Schaffer, R. E. Martin and R. Britton, Direct Heterobenzylic Fluorination, Difluorination and Trifluoromethylthiolation with Dibenzenesulfonamide Derivatives, *Chem. Sci.*, 2018, **9**, 5608–5613.

28 A. Adachi, T. Hashimoto, K. Aikawa, K. Nozaki and T. Okazoe, Difluorination of Heterobenzylic C–H Bonds with *N*-Fluoro-*N*-(Fluorosulfonyl)Carbamate (NFC), *Org. Chem. Front.*, 2023, **10**, 5362–5368.

29 S. Maity, M. A. Lopez, D. M. Bates, S. Lin, S. W. Krska and S. S. Stahl, Polar Heterobenzylic $C(sp^3)$–H Chlorination Pathway Enabling Efficient Diversification of Aromatic Nitrogen Heterocycles, *J. Am. Chem. Soc.*, 2023, **145**, 19832–19839.

30 D. L. Golden, K. M. Flynn, S. Aikonen, C. M. Hanneman, D. Kalyani, S. W. Krska, R. S. Paton and S. S. Stahl, Radical Chlorination of Non-Resonant Heterobenzylic C–H Bonds and High-Throughput Diversification of Heterocycles, *Chem*, 2024, **10**, 1593–1605.

31 M. Kim, E. You, J. Kim and S. Hong, Site-Selective Pyridylic C–H Functionalization by Photocatalytic Radical Cascades, *Angew. Chem., Int. Ed.*, 2022, **61**, e202204217.

32 M. Kaur and J. F. Van Humbeck, Recent Trends in Catalytic sp^3 C–H Functionalization of Heterocycles, *Org. Biomol. Chem.*, 2020, **18**, 606–617.

33 (*a*) Y. Fu, E. E. Zerull, J. M. Schomaker and P. Liu, Origins of Catalyst-Controlled Selectivity in Ag-Catalyzed Regiodivergent C–H Amination, *J. Am. Chem. Soc.*, 2022, **144**, 2735–2746; (*b*) E. E. Zerull, L. E. Vine and J. M. Schomaker, Taming Nitrene Reactivity with Silver Catalysts, *Synlett*, 2021, **32**, 30–44; (*c*) R. J. Scamp, B. Sheffer and J. M. Schomaker, Regioselective Differentiation of Vicinal Methylene C-H Bonds Enabled by Silver-Catalyzed Nitrene Transfer, *Chem. Commun.*, 2019, **55**, 7362–7365; (*d*) J. M. Alderson, J. R. Corbin and J. M. Schomaker, Tunable, Chemo- and Site-Selective Nitrene Transfer through the Rational Design of Silver(I) Catalysts, *Acc. Chem. Res.*, 2017, **50**, 2147–2158; (*e*) J. R. Corbin and J. M. Schomaker, Tunable Differentiation of Tertiary C-H Bonds in Intramolecular Transition Metal-Catalyzed Nitrene Transfer Reactions, *Chem. Commun.*, 2017, **53**, 4346–4349; (*f*) R. Scamp, J. Jirak, I. Guzei and J. M. Schomaker, General Catalyst for Site-Selective $C(sp^3)$-H Bond Amination of Activated Secondary over Tertiary Alkyl $C(sp^3)$-H Bonds, *Org. Lett.*, 2016, **18**, 3014; (*g*) R. Scamp, J. M. Alderson, A. M. Phelps, N. S. Dolan and J. M. Schomaker, Ligand-Controlled, Tunable Silver-Catalyzed C-H Amination, *J. Am. Chem. Soc.*, 2014, **136**, 16720.

34 Y. Cui and C. A. He, Silver-Catalyzed Intramolecular Amidation of Saturated C–H Bonds, *Angew. Chem., Int. Ed.*, 2004, **43**, 4210–4212.

35 M. Huang, J. Paretsky and J. M. Schomaker, Rigidifying Ag(I) Complexes for Selective Nitrene Transfer, *ChemCatChem*, 2020, **12**, 3076–3081.

36 C. M. Alder, J. D. Hayler, R. K. Henderson, A. M. Redman, L. Shukla, L. E. Shuster and H. F. Sneddon, Updating and Further Expanding GSK's Solvent Sustainability Guide, *Green Chem.*, 2016, **18**, 3879–3890.

37 C. G. Espino, P. M. Wehn, J. Chow and J. Du Bois, Synthesis of 1,3-Difunctionalized Amine Derivatives through Selective C–H Bond Oxidation, *J. Am. Chem. Soc.*, 2001, **123**, 6935–6936.

38 D. N. Barman and K. M. Nicholas, Copper-Catalyzed Intramolecular C–H Amination, *Eur. J. Org Chem.*, 2011, 908–911.

39 S. M. Paradine and M. C. White, Iron-Catalyzed Intramolecular Allylic C–H Amination, *J. Am. Chem. Soc.*, 2012, **134**, 2036–2039.

40 S. M. Paradine, J. R. Griffin, J. Zhao, A. L. Petronico, S. M. Miller and M. Christina White, A Manganese Catalyst for Highly Reactive yet Chemoselective Intramolecular C(sp^3)–H Amination, *Nat. Chem.*, 2015, **7**, 987–994.

41 Z. Tian, A. Fattahi, L. Lis and S. R. Kass, Cycloalkane and Cycloalkene C–H Bond Dissociation Energies, *J. Am. Chem. Soc.*, 2006, **128**, 17087–17092.

42 M. Huang, T. Yang, J. D. Paretsky, J. F. Berry and J. M. Schomaker, Inverting Steric Effects: Using "Attractive" Noncovalent Interactions to Direct Silver-Catalyzed Nitrene Transfer, *J. Am. Chem. Soc.*, 2017, **139**, 17376–17386.

43 K. W. Fiori, C. G. Espino, B. H. Brodsky and J. Du Bois, A Mechanistic Analysis of the Rh-Catalyzed Intramolecular C–H Amination Reaction, *Tetrahedron*, 2009, **65**, 3042–3051.

44 I. Nägeli, C. Baud, G. Bernardinelli, Y. Jacquier, M. Moraon and P. Müllet, Rhodium(II)-Catalyzed CH Insertions with {[[(4-Nitrophenyl)Sulfonyl]Imino}phenyl-λ^3-iodane, *Helv. Chim. Acta*, 1997, **80**, 1087–1105.

45 K. W. Fiori and J. Du Bois, Catalytic Intermolecular Amination of C–H Bonds: Method Development and Mechanistic Insights, *J. Am. Chem. Soc.*, 2007, **129**, 562–568.

46 S. H. Park, J. Kwak, K. Shin, J. Ryu, Y. Park and S. Chang, Mechanistic Studies of the Rhodium-Catalyzed Direct C–H Amination Reaction Using Azides as the Nitrogen Source, *J. Am. Chem. Soc.*, 2014, **136**, 2492–2502.

47 V. Bagchi, P. Paraskevopoulou, P. Das, L. Chi, Q. Wang, A. Choudhury, J. S. Mathieson, L. Cronin, D. B. Pardue, T. R. Cundari, *et al.*, A Versatile Tripodal Cu(I) Reagent for C–N Bond Construction *via* Nitrene-Transfer Chemistry: Catalytic Perspectives and Mechanistic Insights on C–H Aminations/Amidinations and Olefin Aziridinations, *J. Am. Chem. Soc.*, 2014, **136**, 11362–11381.

48 K. M. Carsch, S. C. North, I. M. DiMucci, A. Iliescu, P. Vojáčková, T. Khazanov, S.-L. Zheng, T. R. Cundari, K. M. Lancaster and T. A. Betley, Nitrene Transfer from a Sterically Confined Copper Nitrenoid Dipyrrin Complex, *Chem. Sci.*, 2023, **14**, 10847–10860.

49 N. P. van Leest, M. A. Tepaske, B. Venderbosch, J.-P. H. Oudsen, M. Tromp, J. I. van der Vlugt and B. de Bruin, Electronically Asynchronous Transition States for C–N Bond Formation by Electrophilic [Co^{III}(TAML)]-Nitrene Radical Complexes Involving Substrate-to-Ligand Single-Electron Transfer and a Cobalt-Centered Spin Shuttle, *ACS Catal.*, 2020, **10**, 7449–7463.

50 L.-M. Jin, P. Xu, J. Xie and X. P. Zhang, Enantioselective Intermolecular Radical C–H Amination, *J. Am. Chem. Soc.*, 2020, **142**, 20828–20836.

51 M. E. Harvey, D. G. Musaev and J. Du Bois, A Diruthenium Catalyst for Selective, Intramolecular Allylic C–H Amination: Reaction Development and Mechanistic Insight Gained through Experiment and Theory, *J. Am. Chem. Soc.*, 2011, **133**, 17207–17216.